Chapter 2

A Step-by-Step Guide to Single-Subunit Counting of Membrane-Bound Proteins in Mammalian Cells

Mark R.P. Aurousseau, Hugo McGuire, Rikard Blunck, and Derek Bowie

Abstract

Determining the composition and stoichiometry of membrane-bound proteins has been a perennial problem that has plagued biology for a long time. The most recurring issue is that composition and subunit stoichiometry is commonly inferred from bulk biochemical assays that can only shed light on the "averaged" makeup of the protein complex. However, recent studies have been able to circumvent this issue by studying the stoichiometry of *individual* protein complexes. The most common approach has been to express GFP-tagged subunits in *Xenopus laevis* oocytes and then manually count the number of photobleaching steps to report mature protein stoichiometry. Although valuable, an important drawback of this technique is that the strict rules of mammalian protein assembly are not always adhered to in this surrogate expression system. Furthermore, manual counting of bleaching steps is subject to user bias and places practical limits on the amount of data that can be analyzed. In this chapter, we provide a step-by-step account of how we adapted the subunit counting method for mammalian cells to study the composition and stoichiometry of ionotropic glutamate receptors. Using custom-made software, we have automated the entire counting process so that it is much less time consuming and no longer subject to user bias. Given its universality, this methodological approach permits the elucidation of subunit number and stoichiometry for a wide variety of plasma-membrane-bound proteins in mammalian cells.

Key words Single-subunit counting, Single molecule, Automated step detection, Fluorescence spectroscopy, Ionotropic glutamate receptors, Superfolder GFP

1 Introduction

The vast majority of signaling proteins assemble as multimeric complexes including most, if not all, neurotransmitter receptor families found in the vertebrate CNS, such as the ionotropic glutamate receptor (iGluR) and cys-loop receptor families which form tetramers and pentamers, respectively [1, 2]. Insight into the stoichiometry of native receptors has been achieved using ensemble biochemical methods (such as blue native PAGE) or spectroscopic approaches (such as FRET). However, these techniques fall short in that they

Gabriela K. Popescu (ed.), *Ionotropic Glutamate Receptor Technologies*, Neuromethods, vol. 106,
DOI 10.1007/978-1-4939-2812-5_2,

are based on the underlying assumption that stoichiometry is fixed within the entire population. A simple way around this is to study proteins one by one. Consequently, several single-molecule approaches have been developed to determine subunit copy number and stoichiometry of individual protein complexes. Of these, the single-subunit counting method is particularly useful especially when applied to the study of integral membrane proteins.

To achieve this, researchers have used fluorescently labelled proteins and inferred the number of subunits per protein complex by counting the number of photobleaching steps. At the global or macroscopic level, where many fluorophores are present, photobleaching is described by an exponential decay in fluorescence intensity. In contrast, at the single-molecule level, photobleaching produces a rapid steplike decrease in fluorescence intensity as the fluorophore is extinguished. Originally, the concept of photobleaching fluorophores to count subunits was applied to Cy3-labelled nucleotides incorporated into DNA [3] and was later extended to intact cells by Ulbrich and Isacoff to determine the stoichiometry of GFP-tagged ion channels that included NMDA type of iGluR [4].

Subunit counting is commonly performed in *Xenopus laevis* oocytes as it offers fine control of surface expression density as well as an excellent fluorescence signal-to-noise ratio (SNR). However, there are two problems when using this expression system for studying mammalian neurotransmitter receptors. First, this surrogate expression system may not properly assemble mammalian receptors. For example, nicotinic acetylcholine receptors have an altered stoichiometry in *Xenopus laevis* oocytes [5, 6]. Secondly, oocytes express subunits from many neuronal receptor families endogenously, including orthologs of all iGluR subunits [7]. While this potential lack of a fully homogenous population may be ignored in macroscopic measurements, it may significantly influence measurements at the low expression level required for single-molecule observation and become particularly problematic when attempting to interpret subunit counting data. To circumvent these problems, we adapted single-subunit counting to mammalian cells (HEK293). Unlike *Xenopus laevis* oocytes, HEK293 cells do not express iGluRs endogenously but share a number of characteristics with neurons, such as their mRNA expression profile [8].

An important drawback for single-molecule fluorescent imaging is the challenge of achieving a sufficiently high SNR. To realize this, subunit counting is performed using total internal reflection fluorescence (TIRF) microscopy, and fluorescence is detected using highly sensitive cameras. A second major difficulty is to reduce fluorophore-receptor expression density, which we achieved using the protocol described below [9]. From cell culture and transfection to optimizing imaging system components and analysis, we provide a step-by-step procedure describing how to perform

subunit counting experiments in HEK293 cells. Particular emphasis is placed on maximizing the SNR of the system and on reducing fluorophore-receptor expression. We also provide a guide to analyzing raw subunit counting data with *P*rogressive *I*dealization and *F*iltering (PIF) software, an all-in-one analysis suite designed specifically for single-subunit counting [9].

2 Materials

2.1 Cell Culture and Transfection

1. Transfection-grade mammalian expression plasmid designed to express the fusion protein of interest. For iGluR subunits, fusions at the N-terminus should occur after the plasma localization signal. In this chapter, we describe the use of a monomeric version of the superfolder GFP (msfGFP) for subunit counting, but in theory, any fluorescent protein (FP) could be employed as long as it does not readily dimerize. Dimerization could influence the results. An ideal FP should be as bright as possible, be photostable for long periods of time, and have excitation/emission profiles that fall outside the spectra of autofluorescent components of the cell (*see* **Note 1**).
2. HEK293 or HEK293T cells (*see* **Note 2**).
3. Round 35 mm glass-bottom dishes. These can be purchased (MatTek Corp. or WPI) or made by hand in the lab (*see* **Note 3**). It is important to match cover slip thickness (usually #1 or #1.5) to the requirements of the TIRF objective being used.
4. Poly-D-lysine (molecular weight 70,000–150,000 Da) at 10 mg/mL in water. Filter-sterilize the solution with a 0.2 μm filter. Store at −20 °C for months.
5. DMEM (Life Technologies cat. #10564-011) supplemented with 2 % fetal bovine serum (*see* **Note 4**).
6. Phosphate-buffered saline (PBS) containing 100 μM each $MgCl_2$ and $CaCl_2$.

2.2 Sample Fixation

1. 1× and 2× concentrated PBS containing 100 μM each $MgCl_2$ and $CaCl_2$.
2. 20 % EM-grade formaldehyde in H_2O. This can be purchased in small volumes (5–10 mL; Ladd Research Industries) in sealed glass vials and should be stored in the dark at room temperature.

2.3 Imaging

TIRF microscope systems are commercially available or can be built in the lab. The most common type is based on an inverted microscope using a prism-less (or through-the-objective) TIRF setup [10], similar to the setup depicted in Fig. 1. An objective with a numerical aperture larger than 1.42 is required for

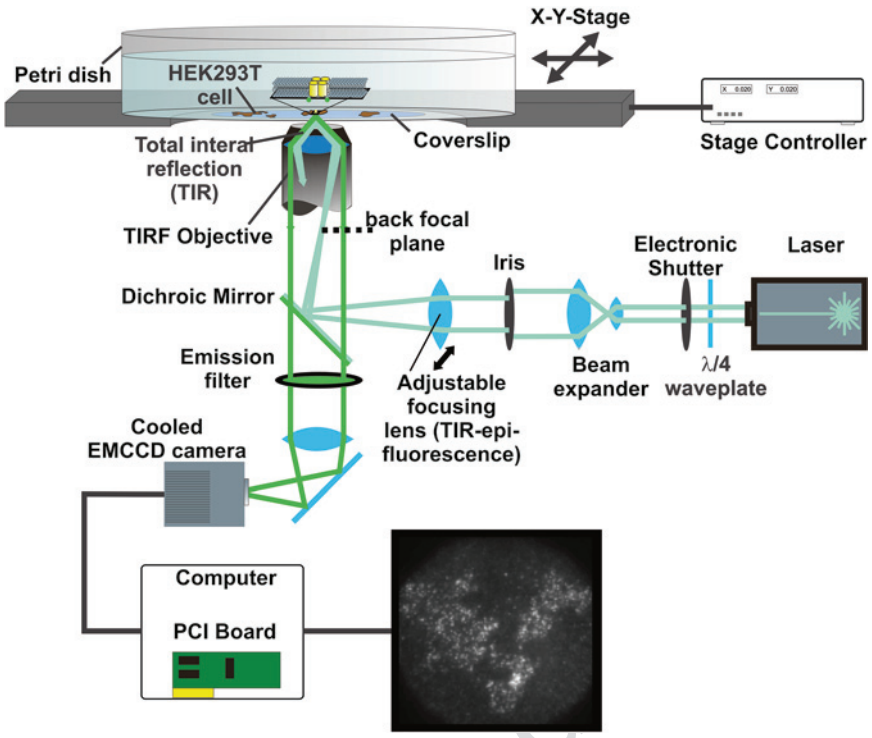

Fig. 1 Schematic representation of a homemade TIRF system. This type of system was used for performing single-subunit counting experiments in mammalian cells as described in [9]

TIRF. These are available from any major microscope manufacturer. Instructions on how to build a TIRF system as well as the theory behind TIRF are outside the scope of this protocol and are available elsewhere [10–12]. Instead, we provide a list of minimum component requirements in addition to the microscope to be able to successfully perform single-subunit counting experiments in mammalian cells.

1. A laser with sufficient power (15–30 mW/wavelength) and low RMS noise (<0.2 % *see* **Note 5**). The wavelength should be matched appropriately to the chosen FP (488 nm for msfGFP).
2. Cooled back-illuminated electron-multiplying CCD camera (EMCCD). A resolution of 128 × 128 pixels is sufficient, but any higher resolution is equally suitable for single-subunit counting experiments. The camera should have low background noise, which is typically achieved using on-chip electron amplifying and cooling; be able to acquire at least 20 frames per second (equivalent to 50 ms/frame); and have a quantum efficiency sufficient for single-molecule observation (typically >80 % in the emission wavelength) (*see* **Note 6**).
3. Darkrooms (e.g., red light room) for sample preparation, fixation, and image acquisition.

3 Methods

3.1 Cell Culture and Transfection

1. Coat 35 mm glass-bottom dishes with poly-D-lysine. Dilute poly-D-lysine stock to a final concentration of 100 μg/mL in water and add 2 mL to each dish. Allow dishes to sit for a minimum of 1 h before rinsing once with PBS.
2. Plate 60,000 HEK293T cells in poly-D-lysine-coated dishes in 2–2.5 mL DMEM containing 2 % FBS (6,230 cells/cm^2). The plating density is chosen to minimize recovery time after plating and to ensure an adequate cell density at the time of image acquisition. The cells are incubated in a humidified atmosphere at 37 °C containing 5 % CO_2.
3. Transfect cells 24–28 h after plating. We use the calcium phosphate method [13] for HEK293T cells. Other transfection methods will likely work, though the amount of transfecting DNA and incubation times will need to be optimized. For expression plasmids driven by CMV promoters, we use between ~50 and 150 ng per dish. For every transfection, it is helpful to prepare multiple dishes, transfecting with a range of quantities of cDNA.
4. Return the cells to the incubator and allow the calcium-DNA precipitate to form and settle for 4 h.
5. Wash the cells twice with PBS and replace with fresh DMEM media. Place back into the incubator and incubate the cells until fixation (*see* **Note 7**).

3.2 Sample Fixation

1. Prepare 4 % EM-grade formaldehyde in PBS on the day of fixation. Mix equal volumes of 20 % EM-grade formaldehyde and 2× concentrated PBS, and then dilute accordingly with 1× PBS to obtain a final concentration of 4 % formaldehyde in 1× PBS. Prepare at least 1.5 mL per transfected dish. This fixation solution should only be used once.
2. All subsequent steps should be performed in the dark or using light outside of the excitation spectrum of the fluorophore. This is to minimize pre-photobleaching of the fluorophores.
3. Wash transfected cells twice with 1× PBS. Add 1.5 mL 4 % formaldehyde solution (from step 1) to each dish and place them at 4 °C for a minimum of 24 h (*see* **Note 8**).
4. After fixation, wash the dishes three times with 1.5 mL cold 1× PBS, leaving 1.5 mL PBS in the dish after the final wash as the imaging solution. At this point the dishes are ready for imaging. Dishes prepared in this way can be stored at 4 °C for weeks prior to imaging.

3.3 Imaging

Due to the diversity in imaging systems able to acquire subunit counting experiments, it would be impossible to write a detailed step-by-step protocol applicable for everyone. Therefore, we concentrated our efforts on providing a general procedure, and

emphasize the need to tailor each system individually to the specific needs of subunit counting.

When it comes to illumination and detection of single-fluorescent molecules, among the most important factors are the short-term stability of the illumination and the signal-to-noise ratio of detection. Particular care should be placed on consistency across experiments and experimental days, especially with respect to sample preparation and illumination intensity. This is vital for determining the probability of observing fluorescence from a FP (p_f) and is the basis for accurately determining the stoichiometry of the protein of interest [9] (see Sect. 3.4.5). This probability is specific to the properties of the fluorophore, imaging system, and depends heavily on the extent of pre-photobleaching. This is why samples are to be prepared in the dark.

3.3.1 *Before Starting: Optimize Illumination and Detection Conditions*

Prior to acquiring subunit counting data for the first time, the user must empirically determine the laser intensity required to (1) observe cells prior to photobleaching ("observation intensity"), and (2) photobleach the fluorophores ("photobleaching intensity"). These values must be optimized for each TIRF imaging system and importantly should not be altered between experiments performed on the same system. Consistency with sample preparation and imaging is absolutely critical when interpreting subunit counting data (see Sect. 3.4.5). The "observation intensity" should be set to minimize pre-photobleaching of the sample as one searches for a cell of interest, but it must also be sufficient to actually be able to visualize the presence of fluorophores on cells. In contrast, "photobleaching intensity" must obviously be sufficient to photobleach fluorophores, but at a rate slow enough to resolve photobleaching steps. For the TIRF system used in [9], a laser power of ~6×10^{-3} μW/μm^2 with a 200 ms exposure was used to search for cells expressing msfGFP-tagged receptors. A continuous laser intensity of ~0.2 μW/μm^2 was used as the "photobleaching intensity." This produced an average fluorescence decay lifetime of about 5 s.

For subunit counting experiments, it is common to collect photobleaching data at rates of 20–33 Hz (30–50 ms/frame) [4, 9, 14, 15]. This acquisition rate gives enough time to accumulate photons and obtain optimal signal strength under photobleaching conditions, while it is still fast enough to minimize missed photobleaching events (steps). Calculating the probability of missing events is presented in [9]. EMCCD gain should be set to a level sufficient to clearly visualize single fluorophores. While this is generally achieved by setting the gain at a relatively high level, saturation leading to premature aging of the camera should be avoided. As a starting point, the Andor iXon+ 860BV camera used in [9] was set to an EMCCD gain of 275.

3.3.2 General Protocol for Collecting Single-Subunit Counting Data

1. Before acquiring data, determine the laser angle required for TIRF. Ensure that the imaging field is illuminated evenly (*see* **Note 9**). For commercial systems, calibrate the TIRF angle offset. This is frequently performed using fluorescent beads on a clean glass-bottom dish. Refer to the system's user manual for these procedures. For homebuilt systems, general TIRF setup procedures have been described previously [11, 12].
2. Verify that laser intensities can be set to the predetermined values set for "observation" and "photobleaching" intensities. For homebuilt systems, this can be done by placing a light power meter in the light path and adjusting the laser power accordingly.
3. Add fluorescence-free immersion oil (Zeiss 518F) to the objective and place a sample dish on the microscope stage.
4. Set EMCCD gain to the predetermined value. Turn on "live mode" and using the "observation intensity" and exposure settings, search the cover slip for a cell to image. Once a cell has been selected, focus on the fluorophores of the cell and promptly turn off the illumination (*see* **Note 10**). Perform this initial step as quickly as possible to minimize pre-photobleaching of the fluorophores.
5. Proceed to set up the system to acquire data. Set the acquisition rate to 50 ms/frame for a duration of ~2.5 min. The duration of the recording need only be as long as it takes to completely photobleach the field. Set the illumination mode to "photobleaching intensity" and start the acquisition. The focus and stage should not have been moved from where it was set in step 4.
6. Monitor the photobleaching progress of the recording. Once fully photobleached, save the recording in Tagged Image File (.tif) format, if possible.

3.4 Analysis

Once subunit counting data has been successfully acquired, the time-resolved fluorescence data can be extracted from the recording. The analysis is relatively straightforward, consisting of simply counting the number of rapid changes in fluorescence intensity (steps) for the duration of the trace. This is repeated for every fluorescent complex on the cell, and for every subsequent recording. In theory, this is relatively simple to perform, but in reality it becomes quite complex and time consuming. The main reason for this added complexity relates to the system SNR. Simply put, the fluorescence signal pertaining to the photobleaching of the fluorophore is hidden in a sea of background noise. Successful extraction of the signal is achieved by applying a series of filtering steps, though even after extensive filtering, fluorescent steps are not necessarily easily distinguishable by eye. Therefore, it becomes essential

that this type of data be analyzed in an objective manner to avoid biasing the results. To get around this, subunit counting analysis is performed using mathematical algorithms implemented in custom software [9]. The PIF software suite was specifically written to automatically complete the analysis of subunit counting data, eliminating any user bias introduced by attempting to manually analyze this type of data. The counting algorithm used by PIF was designed to remain accurate for data acquired from low SNR systems [9]. As a fully automated process, it can be left to sequentially process several recordings, permitting the analysis of thousands of receptor complexes in a couple of hours.

As a complete analysis software suite, PIF automatically identifies and selects pertinent fluorescent spots from the raw recordings, filters the resulting traces to remove background fluorescence, applies a step-counting algorithm to the filtered trace, and finally performs several rounds of quality control to verify the acceptability of the trace and resulting photobleaching steps (Fig. 2). The software performs this procedure for all relevant spots found in the recording and then moves on to the next recording in the loaded dataset. The data are output to a spreadsheet and the results from each of the recordings are compiled to build the step counting distribution. This distribution is used to determine the stoichiometry of the protein of interest (see Sect. 3.4.5). A detailed description of the algorithm used by the software is available

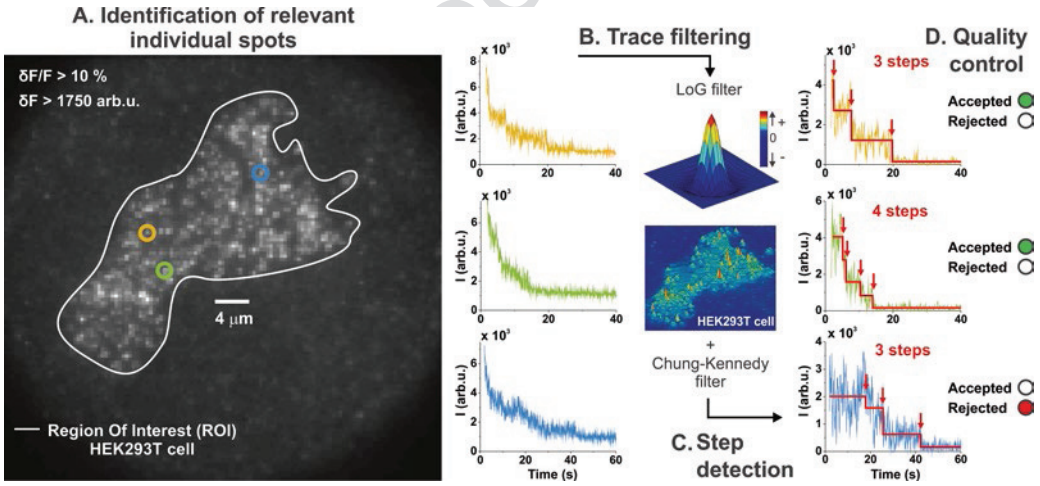

Fig. 2 Summary of the analysis of single-subunit counting data using the software suite PIF. (**a**) Relevant spots are identified and selected from within the user-defined ROI based on specific δF/F and δF criteria. (**b**) Corresponding raw traces from identified spots are filtered using the LoG and Chung–Kennedy filters. (**c**) Steps are detected from the filtered traces and (**d**) are accepted or rejected based upon several criteria of quality control. This figure was adapted with permission from the original, published in The Journal of Biological Chemistry. Hugo McGuire *et al.* Automating Single Subunit Counting of Membrane Proteins in Mammalian Cells. *J Biol Chem*. 2012; 287(43):35912–21.© the American Society for Biochemistry and Molecular Biology

elsewhere [9]. Selecting optimal analysis parameters is an empirical process, and should be done once a suitable control dataset has been collected.

PIF is available upon request (http://tinyurl.com/PIFsoftware) together with a comprehensive user guide describing how to use the program. The user guide also provides a detailed description of each of the various analysis parameters in PIF. Consequently, we will focus on describing the procedures PIF follows to analyze raw subunit counting data. These can be divided into five subsections comprising the selection of a region of interest (ROI), spot detection, filtering noise from traces, step detection, and quality control.

3.4.1 *Selecting a Region of Interest*

Since analysis of subunit counting data should be limited to fluorophores emerging from the cell, it is logical to set a user-defined boundary (a ROI) for analysis. This is done by the user for each recording prior to beginning the analysis by selecting the ROI button from the PIF main screen. Refer to Figs. 2 and 3 for examples of well-defined ROIs (Figs. 2 and 3).

3.4.2 *Spot Detection*

In the context of single-subunit counting, a relevant spot should be one which consists of an individual discernible fluorescent protein. PIF uses two methods to differentiate relevant spots from those pertaining to background fluorescence. The first is based on the area of the spot, a factor largely determined by the point spread function of the imaging system. For example, in a system with a 128×128 pixel EMCCD Andor iXon+ 860BV camera (pixel size 24 μm×24 μm) and a 60× TIRF objective, the relevant spots were defined as covering a maximum region of 3×3 pixels [9]. Second, PIF requires relevant spots to fall within a set of predetermined criteria including

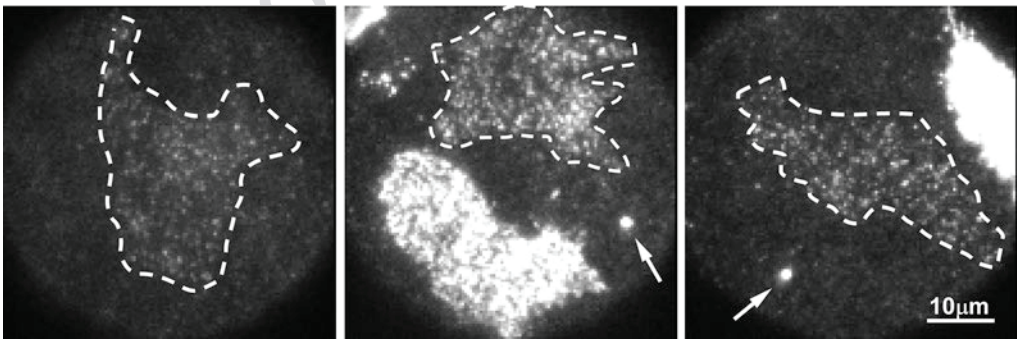

Fig. 3 Example photomicrographs of HEK293T cells expressing msfGFP-tagged GluK2 receptors prior to photobleaching. Each image represents a single 50 ms exposure from the first 0.5 s of recording from three separate experiments. The *dotted lines* delineate cells with optimal fluorophore density for subunit counting experiments. The *middle* and *right images* also contain examples of cells with unacceptably high fluorophore density. These cells are excluded from analysis using the ROI tool in PIF. *White arrows* point to bright fluorescence background spots

intensity threshold and minimum SNR (*see* **Note 11**). This ensures objectivity and consistency when PIF selects spots.

3.4.3 Filtering Noise from Traces

The SNR of subunit counting data acquired from mammalian cells expressing FPs is relatively low. Consequently, the difficult task of extracting relevant fluorescence signals from the raw fluorescence trace is achieved using a series of filters. The first is a Laplacian-of-Gaussian (LoG) convolution filter followed by a Chung–Kennedy filter [16] (*see* **Note 12**).

3.4.4 Step Detection and Quality Control

Photobleaching steps from filtered traces even when acquired from low SNR systems are not always obvious. Consequently, the step detection algorithm in PIF was designed to detect photobleaching steps from this type of noisy data. Details of the algorithm are described in [9]. The accuracy of step detection was determined to be >90 % in systems when SNRs were >2.

In some instances, PIF will count photobleaching steps from spots that do not contain any relevant photobleaching steps. These traces are often derived exclusively from background fluorescence. To exclude these traces from the final analysis, PIF was programmed to run through a series of quality control steps that are applied to each trace before accepting it. The basis for quality control is essentially a set of criteria that each trace must pass. The parameters for each criterion were optimized to avoid rejecting pertinent traces. A trace must satisfy all the following criteria:

(a) Chi-squared (χ^2) goodness-of-fit evaluation ($\chi^2 < 1.5$) and must be less than the χ^2 value of a counter-fit [17]

(b) Signal-to-noise (mean step size/noise of the trace) > 2.5

(c) Time required to bleach n fluorophores: $t_{\text{last step}} < \tau \cdot \ln(1 - p^{1/n})$, where $p = 0.90 - 0.98$, and τ is the overall average of decay

(d) Maximal step amplitude: max. ~3 times the amplitude of the average step size obtained from a step amplitude distribution

3.4.5 Analyzing the Step Distribution

Stoichiometric information is extracted from the final step distribution that is output by PIF. For proteins with fixed stoichiometry or oligomerization, this final probability histogram generally follows a binomial distribution (or sum of binomials, see Fig. 4). Other possibilities include a Poisson distribution or a mixture of binomial and Poisson distributions (*see* **Note 13**). Since this type of distribution is subject to the probability that a fluorophore is indeed fluorescent (p_f), the two main contributors to its value are the amount of pre-photobleaching prior to image acquisition and the likelihood that an FP has folded and matured correctly to become fluorescent. If samples are prepared in a consistent manner with respect to light exposure (described in Sects. 3.1 and 3.2), then any effect of pre-photobleaching should be negligible.

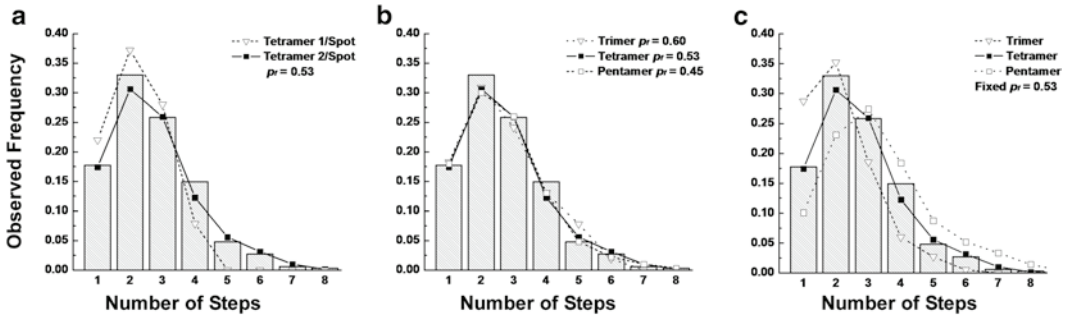

Fig. 4 Frequency distributions of a control subunit counting experiment performed on homotetrameric msfGFP-tagged GluK2 receptors (n=1,312 spots) to determine the p_f of the system. (**a**) The observed step distribution is best fit with the sum of two binomial distributions, indicating that two receptor complexes can be situated in the same resolvable spot, below the diffraction limit of the system. (**b**) Distinct binomial distributions (third, fourth, and fifth orders for trimer, tetramer, and pentamer, respectively) can be equally well fit to the dataset if p_f is allowed to vary. (**c**) When p_f is fixed, third- and fifth-order binomials clearly do not fit the observed distribution. Data were published in The Journal of Biological Chemistry. Hugo McGuire *et al.* Automating Single Subunit Counting of Membrane Proteins in Mammalian Cells. *J Biol Chem*. 2012; 287(43):35912–21.© the American Society for Biochemistry and Molecular Biology

The probability of counting k photobleaching steps for an oligomer containing n subunits can then be represented as

$$p(k) = \frac{n!}{k!(n-k)!} p_f^k \left(1 - p_f^{n-k}\right)$$

Using this equation to fit an observed step distribution of an oligomer with a fixed and known stoichiometry, it is possible to extract the probability that a given FP is fluorescent (p_f). However, since p_f and n are initially unknown, stoichiometric information cannot be reliably extracted because several combinations of p_f and n will fit the data (Fig. 4b). To circumvent this issue, we estimated p_f experimentally using a control dataset of two multimeric proteins with known subunit stoichiometry, namely homomeric msfGFP-tagged GluK2 and glycine α1 (GlyRα1) receptors which assemble as tetramers and pentamers, respectively [9]. Using this approach, we estimated p_f to be 0.53 in both cases, greatly simplifying the interpretation of the observed step distribution (Fig. 4c). Interestingly, a general inference model has also been developed that uses a complementary approach by accurately estimating p_f confidence [18]. Several factors seem to influence p_f including the temperature and the type of expression system, but p_f remains constant for a given FP if experiments are prepared and imaged under the exact same conditions [9].

If more than one fixed oligomerization state exists, the final step distribution will be a sum of binomial distributions. For example, this applies if a significant proportion of identified spots contain two or more fluorescent complexes [9]. These cases are

easily recognized in control datasets where traces will contain more steps than the known number of subunits (Fig. 4a), but they become challenging to interpret when the stoichiometry is unknown. As a consequence, the stoichiometry can only be reliably extracted by first determining the value for p_f.

4 Notes

1. Although the superfolder GFP has been described as a monomer [19], we incorporated a well-known monomerization mutation (V206K) [20]. Venus [21] and mNeonGreen [22] are two attractive alternatives to msfGFP because of their superior brightness and yellow-shifted excitation profiles. The shift to longer wavelengths is advantageous for cellular imaging because cellular autofluorescence is excited less at these wavelengths, leading to reduced background fluorescence and increased SNR. As such, red-shifted fluorophores such as mCherry may seem attractive for the purposes of subunit counting, but the dimness (low quantum yield) and rapid photobleaching of mCherry have limited its use as a receptor location marker [23, 24]. Additionally, the surface trafficking of iGluRs fused N-terminally to mCherry is perturbed in HEK293T cells (unpublished observation), making this fluorophore a poor choice for single-subunit counting of iGluRs.
2. Other mammalian cell lines may be suitable for fluorescent subunit counting, but HEK293T cells were chosen for ease of transfection as well as their reliable expression of iGluRs. Also, note that vectors containing an SV40 origin of replication are replicated episomally in cell lines harboring the SV40 large-T antigen (i.e., HEK293T cells). This feature is not desirable when attempting to control receptor expression density. One way around this is to simply remove the SV40 origin of replication from the expression vector.
3. Homemade 35 mm glass-bottom dishes can be suitable for single-molecule imaging provided that they are prepared carefully. Cover slips need to be extensively cleaned to sufficiently reduce background fluorescence. This is done by first wiping each cover slip with a lint-free wipe soaked in Alconox. Then, in a solvent-resistant glass jar, sonicate cover slips at 37 kHz for 30 min at 50 °C with Alconox. Repeat this sonication step twice more with anhydrous ethanol. Before and after each sonication run, rinse the cover slips with ultrapure (Type I) H_2O. Prepare standard 35 mm plastic culture dishes to accept a cleaned glass cover slip by first melting a pilot hole using a red-hot nail or a screw. Then, using a conical bit attached to a standard hand drill, drill a hole slightly smaller than the cover

slip. Glue the cover slip (from the top) with a liquid adhesive/sealant (Sylgard 184 silicone elastomer kit) following the product instructions. Sterilize poly-D-lysine-coated dishes under UV light before culturing.

4. Media type and FBS content are optimized for single-subunit counting experiments performed on the HEK293T cell line. These conditions cannot necessarily be extended to other mammalian cell lines/types. Limiting FBS content to between 1 and 3 % restricts the rate of cell division and promotes cell flatness on the cover slip, increasing the area of the cell in contact with the surface. This is advantageous for reducing the apparent fluorophore-receptor density required for single-molecule imaging.
5. Use of a polarized light output, such as that of a laser, has an important drawback for single-molecule imaging of fixed FPs. The emitted fluorescence intensity of an FP is affected by the relative orientation of its electric dipole versus the electric field of the laser beam. Consequently, restricting movement of the FP by fixation could significantly influence the fluorescence intensity of the fluorophore, leading to greater variability in the amplitudes of photobleaching step. This can be problematic when setting a specific step size criterion, as is required by PIF for step detection (see Sect. 3.4.4). This potential problem is averted by simply placing a quarter-wave plate ($\lambda/4$) in the illumination path to produce a circular polarization (Fig. 1).
6. Contrary to standard CCD cameras, EMCCDs contain a solid-state electron-amplifying system to augment the collected signal prior to the addition of any readout noise, greatly enhancing the SNR. A key feature of many EMCCDs is the ability to "frame transfer." This allows the camera to continue accumulating photons for the current frame while simultaneously processing the data from the previously acquired frame. This architecture permits acquisition rates of up to 500 frames per second for some models and is highly recommended for performing single-subunit counting experiments.
7. The duration of this incubation period is critical for determining the final fluorophore-receptor density and must be empirically optimized for each receptor subtype of interest. We found that 16–18 h is ideal for the GluK2 receptor as well as the GlyRα1 receptor [9]. At minimum, the duration of this incubation period must account for the time it takes the receptor to traffic to the surface of the cell. This is important given that FPs located intracellularly are readily detected, even under TIRF illumination.
8. It is crucial that fluorophores are completely immobile for successful subunit counting of the receptor complex. Consequently, it was empirically determined that complete immobilization of

tagged-receptors occurs only after at least 24 h in 4 % formaldehyde at 4 °C. Common protocols for HEK293 cells describing fixation durations of 5–20 min at room temperature do not adequately immobilize the tagged receptors. Fluorophore movements are readily detectable at the single-molecule level. A telltale sign of incomplete fixation is the obvious movement of fluorophores about the surface of the cell as well as into and out of the TIRF excitation field. This movement is best described as "twinkling stars." Recordings with this phenotype should be excluded from analysis because it is difficult to distinguish between photobleaching and a movement out of the TIRF excitation field.

9. Uniformity in the excitation intensity over the illuminated region is critical to reduce variability in the subunit counting data. This is generally taken care of in commercial TIRF systems, but must be properly adjusted for homemade systems. Unaltered laser beams tend to only illuminate a small region of the sample with an intensity distribution approximated by a Gaussian profile. Consequently, to produce a uniform illumination of the entire sample, a beam expander combined with an adjustable iris is placed in the light path (Fig. 1). The beam expander spreads the Gaussian beam and the iris is set to retain a small fraction of the spread beam. The most intense section of the beam able to illuminate the entire field of the camera should be kept. These modifications are able to produce a sufficiently uniform excitation field, but they come at the cost of total laser intensity. Therefore, for this type of setup, a relatively high-power laser is required (>15–30 mW). Alternatively, uniform field illumination can also be achieved using commercially available circular beam diffusers.

10. Even under optimized illumination conditions, it may be difficult to visualize the presence of fluorophores on a transfected cell, especially if receptor density is within the desired range. When first learning to perform this technique, it may be helpful to switch to "photobleaching intensity" when the observer believes that he or she is looking at a cell. Although cells visualized in this way cannot be used for analysis due to extensive pre-photobleaching, this serves the purpose of training the user to identify cells with sufficiently low densities under low-intensity illumination. For comparison, Fig. 3 provides several examples of what cells should be expected to look like under photobleaching illumination when suitable receptor densities for subunit counting are imaged (Fig. 3). Frequently, cells with suitable fluorophore density are found adjacent to cells that have high fluorescence densities (Fig. 3, middle and right panels). In these cases, it is impossible to photobleach one without the other. This is one of the reasons the ROI tool was incorporated into the PIF analysis software.

11. In principle, selection of relevant spots could be achieved using a set intensity threshold alone. However, in some circumstances, areas are bright because of high background fluorescence. Having to additionally satisfy a minimum signal-to-noise ratio value eliminates the problem, preventing the selection and subsequent analysis of spots consisting primarily of background fluorescence.
12. The LoG filter is of the following form:

$$\mathrm{LoG}(x,y) = \left[1 - \frac{x^2 + y^2}{2\sigma^2}\right] \mathrm{e}^{-\frac{x^2+y^2}{2\sigma^2}}$$

where σ is the Gaussian width. For setting that value, we recommend fitting all spots with a two-dimensional Gaussian function and choosing the peak maxima of the Gaussian width distribution. To apply the LoG filter, its corresponding matrix (from the eq. above) can simply be centered over any spot of interest, as the elements of both filter and the spot matrix will be multiplied with each other. The sum of the elements of the resulting matrix is the filtered fluorescence signal. The size of the filter and spot matrix should be kept constant and slightly larger than the region covered by the spots. For instance, if the intensity is mostly distributed within one pixel (the center spot pixel), a 3×3 matrix should be sufficient. If the spot intensity is spread to a center pixel and one neighbor, a 5×5 matrix would be appropriate for the spot and filter matrix.
13. In cases where a fixed stoichiometry cannot be associated to a dataset, it may indicate that these subunits are randomly distributed oligomers about an average subunit number (λ). These can be described by a Poisson distribution as follows:

$$p(k) = \mathrm{e}^{-\lambda} \frac{\lambda^k}{k!}$$

Such a distribution has been described for the case of low concentrations of Cry1Aa toxin [14].

References

1. Corringer P-J et al (2012) Structure and pharmacology of pentameric receptor channels: from bacteria to brain. Structure 20(6): 941–956
2. Traynelis SF et al (2010) Glutamate receptor ion channels: structure, regulation, and function. Pharmacol Rev 62(3):405–496
3. Park M et al (2005) Counting the number of fluorophores labeled in biomolecules by observing the fluorescence-intensity transient of a single molecule. Bull Chem Soc Jpn 78(9):1612–1618
4. Ulbrich MH, Isacoff EY (2007) Subunit counting in membrane-bound proteins. Nat Methods 4(4):319–321

5. Krashia P et al (2010) Human alpha3beta4 neuronal nicotinic receptors show different stoichiometry if they are expressed in Xenopus oocytes or mammalian HEK293 cells. PLoS One 5(10):e13611
6. Sivilotti LG et al (1997) Recombinant nicotinic receptors, expressed in Xenopus oocytes, do not resemble native rat sympathetic ganglion receptors in single-channel behaviour. J Physiol 500(Pt 1):123–138
7. Schmidt C, Klein C, Hollmann M (2009) Xenopus laevis oocytes endogenously express all subunits of the ionotropic glutamate receptor family. J Mol Biol 390(2):182–195
8. Shaw G et al (2002) Preferential transformation of human neuronal cells by human adenoviruses and the origin of HEK 293 cells. FASEB J 16(8):869–871
9. McGuire H et al (2012) Automating single subunit counting of membrane proteins in mammalian cells. J Biol Chem 287(43):35912–35921
10. Axelrod D (2003) Total internal reflection fluorescence microscopy in cell biology. Methods Enzymol 361:1–33
11. Mattheyses AL, Simon SM, Rappoport JZ (2010) Imaging with total internal reflection fluorescence microscopy for the cell biologist. J Cell Sci 123(Pt 21):3621–3628
12. Johnson DS, Jaiswal JK, Simon S (2012) Total internal reflection fluorescence (TIRF) microscopy illuminator for improved imaging of cell surface events. Curr Protoc Cytom Chapter 12:Unit 12.29
13. Chen C, Okayama H (1987) High-efficiency transformation of mammalian cells by plasmid DNA. Mol Cell Biol 7(8):2745–2752
14. Groulx N et al (2011) Single molecule fluorescence study of the Bacillus thuringiensis toxin Cry1Aa reveals tetramerization. J Biol Chem 286(49):42274–42282
15. Das SK et al (2007) Membrane protein stoichiometry determined from the step-wise photobleaching of dye-labelled subunits. Chembiochem 8(9):994–999
16. Chung SH, Kennedy RA (1991) Forward-backward non-linear filtering technique for extracting small biological signals from noise. J Neurosci Methods 40(1):71–86
17. Kerssemakers JW et al (2006) Assembly dynamics of microtubules at molecular resolution. Nature 442(7103):709–712
18. Hines KE (2013) Inferring subunit stoichiometry from single molecule photobleaching. J Gen Physiol 141(6):737–746
19. Pedelacq J-D et al (2006) Engineering and characterization of a superfolder green fluorescent protein. Nat Biotechnol 24(1):79–88
20. Zacharias DA et al (2002) Partitioning of lipid-modified monomeric GFPs into membrane microdomains of live cells. Science 296(5569): 913–916
21. Nagai T et al (2002) A variant of yellow fluorescent protein with fast and efficient maturation for cell-biological applications. Nat Biotechnol 20(1):87–90
22. Shaner NC et al (2013) A bright monomeric green fluorescent protein derived from Branchiostoma lanceolatum. Nat Methods 10(5):407–409
23. Yu Y et al (2009) Structural and molecular basis of the assembly of the TRPP2/PKD1 complex. Proc Natl Acad Sci U S A 106(28): 11558–11563
24. Nakajo K et al (2010) Stoichiometry of the KCNQ1-KCNE1 ion channel complex. Proc Natl Acad Sci U S A 107(44):18862–18867